An experimental verification of a percolation model for RuO_2-glass thick resistive films

1991 J. Phys.: Condens. Matter 3 7015

(http://iopscience.iop.org/0953-8984/3/36/007)

J. Phys.: Condens. Matter 3 (1991) 7015–7026. Printed in the UK

An experimental verification of a percolation model for RuO_2–glass thick resistive films

Krzysztof Bobran and Andrzej Kusy
Department of Electrical Engineering, Technical University of Rzeszów, Wincentego Pola 2, 35-959 Rzeszów, Poland

Received 3 January 1991, in final form 29 April 1991

Abstract. We present the results of our experimental work concerning the sheet resistance, $R_\square$, temperature characteristics of resistance and relative power spectral density of $1/f$ noise, S, versus the volume fraction of conducting component, v, for RuO_2–glass composites. We eliminate the contributions of contact-film–resistive-film interfaces to the measured characteristics. We find that the composites investigated can be mapped onto the three-component 3D random resistor network (RRN) formed from well conducting metallic bonds, poorly conducting metal–insulator–metal (MIM) bonds and those not conducting. We provide the physical interpretation of the network's parameters: h_g, h_s, b_1, i.e. the ratio of conductances of poorly and well conducting bonds, the ratio of their $1/f$ noise relative power spectral densities and the fraction of metallic bonds in the set of all conducting bonds, respectively. The electrical transport characteristics of RuO_2–glass thick resistive films are interpreted with the help of bicritical behaviour of such a percolation network. We find qualitative agreement between $S(R_\square)$ experimental data for a certain region of v and that from 3D RRN computer simulations using the Monte Carlo real space renormalization group algorithm.

1. Introduction

The thick film resistor is the structure made from conductive and resistive pastes by screen-printing and firing them consecutively on a ceramic substrate to form the contact films and thick resistive film (TRF), respectively. The properties of a thick film resistor are dominated by the features of the TRF. The RuO_2–glass TRFs have often been described as metal–insulator composites (Vest 1975, Pike 1978, Kusy 1979, Carcia *et al* 1983, Listkiewicz and Kusy 1985, Kubovy 1986, Kubovy 1988). Hence 3D binary random resistor networks (RRNs) were first considered as models for them. The characteristics of the resistance R versus the concentration of conducting component x for such a network is described by the equation $R \propto (x - x_c)^{-t}$, where x_c is the critical concentration of conducting component and t is the critical conductivity exponent. It has been reported that $t \simeq 2.0$ for discrete lattice percolation (Stauffer 1985) and $t \in \{2.0, 2.5\}$ for continuum percolation (Halperin *et al* 1985, Feng *et al* 1987). A similar equation with critical exponent κ has also been used to describe the $1/f$ noise relative power spectral density, $\langle(\delta R)^2\rangle/(\Delta f R^2) \equiv S \propto (x - x_c)^{-\kappa}$ of 3D binary RRNs, with $\kappa \simeq 1.5$ for discrete lattice (Kolek and Kusy 1988), $\kappa \simeq 4.8$ for inverted random void and $\kappa \simeq 5.5$ for random void percolations (Tremblay *et al* 1986, Tremblay *et al* 1989). Since both R and S are power

0953-8984/91/367015 + 12 $03.50

law functions of $(x - x_c)$ then for a given percolation network the S versus R dependence is a straight line of slope $w = \kappa/t$ on a log–log plot.

Great effort has been made by researchers to fit the experimental data by the power laws $R \propto (v - v_c)^{-t}$ and $S \propto (v - v_c)^{-\kappa}$, with x, x_c from RRN corresponding to v, v_c, the volume fraction and critical volume fraction of conducting component in TRFs. The values of t from 2 to 7 that have been found for RuO_2–glass TRFs (Pike 1978, Kusy 1979, Carcia *et al* 1983, Inokuma *et al* 1984, Listkiewicz and Kusy 1985, Kubovy 1986, Bobran 1989) are often evidently greater than those predicted by binary percolation theory. Furthermore, some experimental $1/f$ noise data show qualitatively different behaviour as S versus $(v - v_c)$ is not monotonic (Kusy 1979, Inokuma *et al* 1985, Bobran 1989). For various TRFs, S versus R has been directly studied experimentally (Ringo *et al* 1976, deJeu *et al* 1981, Müller and Wolf 1988). However, no clear confirmation of the straight line behaviour predicted by the theory has been found.

To improve understanding of the experimental data for RuO_2–glass TRFs, the three-component 3D RRN as a TRF model has been proposed and studied recently (Carcia *et al* 1983, Kusy and Listkiewicz 1988, Kusy 1988, Kusy and Kolek 1989, Bobran and Kusy 1989, Kolek 1989, Listkiewicz 1989). This is the network built on a simple cubic lattice of sites in which bonds between any pair of two nearest-neighbour sites are occupied in a random way by one of the three conductances: $g = 0$, $g = g_C$ and $g = g_B$. In the papers of our group cited above it has already been indicated that $R(v - v_c)$, $S(v - v_c)$ and $R(T)$, where T denotes the temperature, for RuO_2–glass TRFs can be explained within the framework of a three-component RRN.

The purpose of this paper is to report an improved experimental verification of the three-component RRN as a model of RuO_2–glass TRFs. First we state that a RuO_2–glass TRF is not just the macroscopically homogeneous composite realized by the properly designed procedure of mixing metallic and glass powders. It is so mainly due to the interactions on the resistive-film–conductive-film interfaces (Cattaneo *et al* 1977, Paszczyński 1985, Yamaguchi and Kageyama 1988, Bobran and Kusy 1989). We demonstrate the existence of these types of interactions and their effects on $R(v)$ and $S(v)$ characteristics. We introduce the three-component RRN with its bicritical behaviour, i.e. with the existence of two critical points: one corresponding to the onset of electrical conduction and the other to the formation of the metallic cluster spanning the electrodes. We verify its use in describing $R(v)$ and $S(v)$ curves for the parts of films free of the contact effects. The set of $R(T)$ characteristics presented in the paper help us to identify the second percolation threshold while the first one is evaluated from $R(v)$ dependence. We develop our model, described in earlier papers, by introducing b_1, the fraction of metallic bonds in the set of all conducting bonds, as a function of x, $b_1(x)$, which has been taken as constant until now. We think this is a physically more acceptable way of modelling our composite.

2. Experimental procedure

We subjected to examination the series of nine resistive pastes that consisted of 24 m^2/g RuO_2 powder (the evaluated mean grain size $\sigma \simeq 400$ Å) as a conducting component and 2.4 m^2/g ($\sigma_g \simeq 0.55$ μm) lead borosilicate glass powder both dispersed in terpineol and ethyl cellulose. The volume fraction v of RuO_2 was varied in the range 0.02 to 0.32. The details of the technological process of obtaining pastes and then the appropriate thick resistive films have been presented elsewhere (Bobran 1989). We have measured

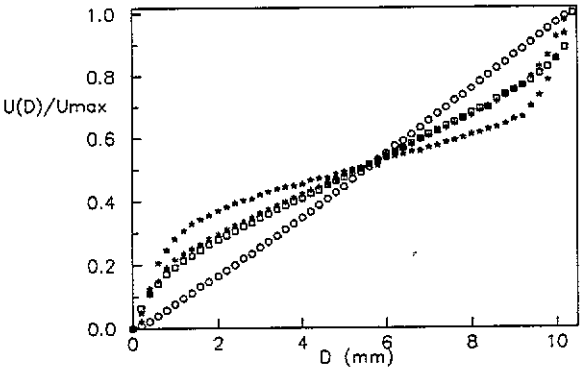

Figure 1. The examples of potential distributions along the biased films for 4 chosen TRFs of v: (○) 0.32; (*) 0.17; (★) 0.08; (□) 0.05. The potential $U(D)$ measurements were done at every 50 μm distance D starting from the grounded electrode. U_{max} is the value of the biasing voltage.

the sheet resistance $R_\square$, the relative $1/f$ noise power spectral density (relative noise) S and the temperature characteristics of resistance for these composites with prior checking of the potential distributions along the biased TRFs.

The potential distributions were measured with the aid of a potential point probe moved along the film by a micrometer screw (Cattaneo *et al* 1977). Some illustrative results are presented in figure 1. It can be seen that for a low resistance film (i.e. high RuO_2 content) a roughly straight line was obtained while for higher resistances three distinct regions, each with roughly straight line dependence are visible: the centre one and two others close to the contact films. The first region corresponds to a composite material that consists of a volume v of RuO_2 powder and $(1 - v)$ of glass powder. The two other regions correspond to contact modified parts of the film (CMPF). The Pd–Ag contact causes the resistivity increase within the CMPFs in spite of silver ions migrating from the contact films to these regions (Cattaneo *et al* 1977). Some recent investigations of Yamaguchi and Kageyama (1988) confirm the results obtained and offer an explanation of this phenomenon. They state that the increase in electrical resistivity is caused by the decreased concentration of RuO_2-associated charge carriers in CMPF due to their interactions with silver ions. The lengths of CMPFs for our samples were in some cases as large as 1–2 mm. The increase in resistivity of regions close to the contact was different for samples of different v (figure 1). For samples of high sheet resistance values, i.e. the films of low RuO_2 content, the potential probe method described turned out not to be applicable. This was related to the thin glassy layer originating on the surface of such films. Therefore, in the case of films having a resistance greater than 10 MΩ we measured the potential distribution on potential legs along the film (see the test pattern in figure 2(a)). To obtain these measurements we used an electrometer. The set of curves obtained was used to calculate $R_\square$ for the central parts of films as well as the lengths L_c of CMPFs. It was stated that CMPFs cause the relative sheet resistance changes down to -0.8.

Our technique of noise measurement was developed on the basis of the previous papers on this topic (Rhee and Chen 1978, Demolder *et al* 1980, Demolder *et al* 1983, Mantese and Webb 1985, Bobran 1990). We consider two components of current noise in the structures investigated: (i) generated in CMPF and (ii) generated in the central part of TRF. We separate them in a similar manner as did Rhee and Chen (1978) with the contact noise and the bulk noise for their TRFs. However, to maintain the proper biasing of our samples of resistance ranging from $10^1\ \Omega$ up to $10^9\ \Omega$ we used the measuring circuit shown in figure 2(a). This is a Wheatstone bridge circuit excited with DC current. The central current tap of the sample was grounded. Thus two adjacent arms of the

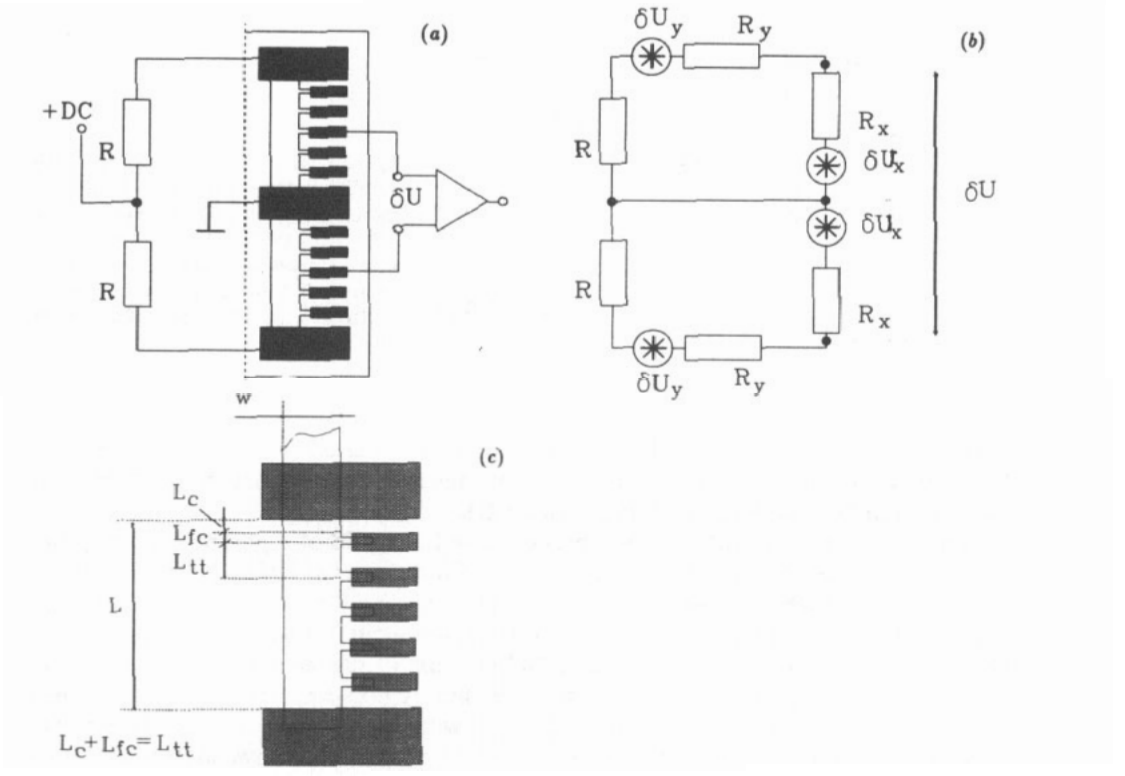

Figure 2. (*a*) Test pattern as connected into the $1/f$ noise measuring set-up. It consists of two identical resistors with the central and two extreme current taps and five pairs of potential legs along the resistive film symmetric in relation to the central tap. The output signal δU of the circuit was amplified by a FET preamplifier (preceded by an impedance transformer for low resistance samples) and wide band amplifier all UNIPAN Model 233 and then observed on the oscilloscope connected in parallel with the Quan-Tech Wave Analyser Model 304TDL to obtain the measurement. (*b*) Equivalent circuit for the noise of the Wheatstone bridge of figure 2(*a*). R is a wire wound resistor, δU the analysed output signal. R_x, δU_x are resistance and voltage fluctuations corresponding to the TRF part between the grounded current electrode and actual potential probe while R_y, δU_y are the respective values for the remaining part of the TRF. (*c*) Definitions of geometrical parameters of the TRF investigated. L_c is the length of CMPF, L_{tt} is the distance between two consecutive electrodes and $L_{fc} = L_{tt} - L_c$.

bridge were formed from the resistive film divided into two symmetrical parts. Two other arms of the bridge were built using two wire-wound resistors of resistance R. It is seen from figure 2(*a*) that due to the balance of the bridge a DC component close to zero is always obtained at the input of the amplifying system. There are two benefits from this. Firstly, we could use high voltages to bias high resistance samples and secondly, in the case of low resistance samples, we could apply the impedance transformer to lower the system noise. We followed the measuring procedure as described below.

For a given TRF we measured the RMS values of voltage fluctuations, $\sqrt{\langle(\delta U)^2\rangle}$, over a fixed frequency bandwidth, Δf, at a given frequency f on consecutive pairs of potential legs. We always checked the $1/f$ behaviour of the noise studied by plotting $\langle(\delta U)^2\rangle$ versus f. Using a log–log scale we always obtained straight lines. The calculated slope of these

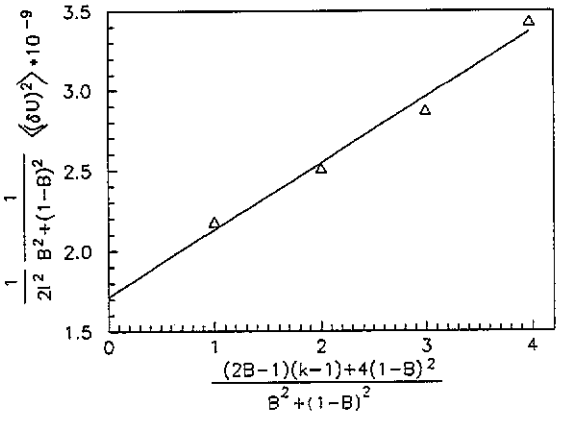

Figure 3. Examples of results of absolute noise measurements for a RuO_2–glass composite of $v = 0.17$. The extrapolation of the line obtained by the least squares linear fit to $X = 0$ gives the intersection value: $Y = \langle(\delta R_c)^2\rangle + \langle(\delta R_{fc})^2\rangle$, while its slope is $\langle(\delta R_{tt})^2\rangle$ (see (3)). The data points were obtained by successive noise measurements starting from the potential leg numbered $k = 2$. The leg $k = 1$ was omitted in the plot because it was obscured by the CMPF noise. The fact that data points do not lie strictly on the line may be attributed to the fact that the point for $X = 4$ possible already lies in the CMPF.

lines, α, was in the range $-1.31 \leqslant \alpha \leqslant -0.85$. In addition we verified the dependence of $\langle(\delta U)^2\rangle$ versus the DC biasing voltage. On a log–log scale we obtained straight lines with a positive slope γ in the range $1.96 \leqslant \gamma \leqslant 2.1$. Thus typical $1/f$ noise behaviour has been identified. We took the values of the pre-exponential factors of $\langle(\delta U)^2\rangle$ versus f as a measure of voltage fluctuations at $f = 1$ Hz for further analysis.

From the equivalent circuit for noise shown in figure 2(b) and using the parameters defined in figure 2(c) we calculated the power spectrum of resistance fluctuations (absolute noise) of TRFs. For a given frequency and frequency bandwidth we can write (see figure 2(b)):

$$\tfrac{1}{4}\langle(\delta U)^2\rangle = [(R + R_y)/(R + R_y + R_x)]^2\langle(\delta U_x)^2\rangle + [R_x/(R + R_y + R_x)]^2\langle(\delta U_y)^2\rangle. \tag{1}$$

Assuming the lack of correlations between the noises originating in TRF parts of lengths L_c, L_{fc}, L_{tt} (see figure 2(c)) we divide $\langle(\delta U_x)^2\rangle$ and $\langle(\delta U_y)^2\rangle$ into the following parts:

$$\begin{aligned}\langle(\delta U_x)^2\rangle &= I^2[\langle(\delta R_c)^2\rangle + \langle(\delta R_{fc})^2\rangle + (k-1)\langle(\delta R_{tt})^2\rangle] \\ \langle(\delta U_y)^2\rangle &= I^2[\langle(\delta R_c)^2\rangle + \langle(\delta R_{fc})^2\rangle + (5-k)\langle(\delta R_{tt})^2\rangle].\end{aligned} \tag{2}$$

Here I is the DC current flowing through the resistive film, $\langle(\delta R_{tt})^2\rangle$, $\langle(\delta R_{fc})^2\rangle$ are the absolute noises of the TRF's parts of lengths L_{tt} and L_{fc} free of contact effects, $\langle(\delta R_c)^2\rangle$ is the absolute noise of the CMPF and k is the number of the actual potential leg starting from the grounded current tap. Putting (1) and (2) together we obtain:

$$\frac{1}{2I^2(B^2 + (1-B)^2)}\langle(\delta U)^2\rangle = \langle(\delta R_c)^2\rangle + \langle(\delta R_{fc})^2\rangle + \frac{(2B-1)(k-1) + 4(1-B)^2}{B^2 + (1-B)^2}\langle(\delta R_{tt})^2\rangle \tag{3}$$

where $B = (R + R_y)/(R + R_y + R_x)$. The parameter B can be called the attenuation factor of the measured signal. It reaches a maximum value equal to 1 (no attenuation) when the sum of the resistances $(R + R_y)$ far exceeds the resistance R_x. Figure 3 shows an example of experimental data obeying (3) and explains the method of $\langle(\delta R_{tt})^2\rangle$ calculation as the slope of the straight line obtained. It also shows the proportionality of

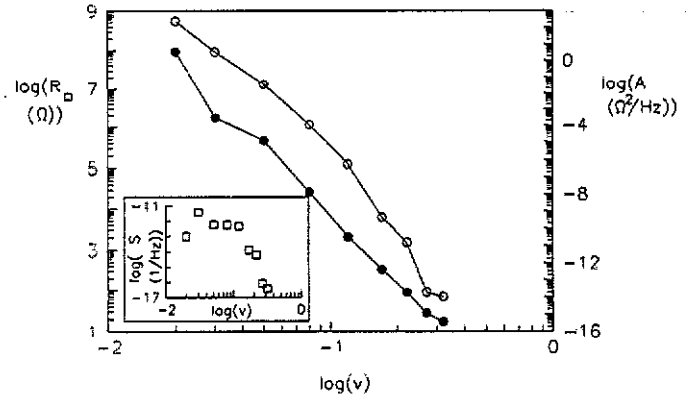

Figure 4. The sheet resistance $R_\square$ (●) and absolute noise A (○) versus volume fraction of conducting component v for RuO_2–glass composites. The relative noise S (□) versus v is shown in the inset. The solid lines are drawn to guide the eye.

the absolute noise, and the inverse proportionality of the relative noise, $S \equiv \langle(\delta R_{tt})^2\rangle/(R_\square L_{tt}/w)^2$, to the volume of the sample. CMPFs cause the changes in S (related to the S calculated from uncorrected values of $\langle(\delta R_{tt})^2\rangle$ and $R_\square$) from -0.8 to $+10$ depending on v. The maximum change considered above has been obtained for the TRF having the greatest CMPF contribution to its sheet resistance.

The temperature characteristics of resistance for TRFs of v ranging from 0.05 to 0.32 have been measured from the liquid nitrogen temperature to +125 °C. The temperature has been controlled by a Pt-100 type sensor.

3. Results and discussion

First, following the methods described in the previous section, we have measured the characteristics of $R_\square$, absolute A and relative S noises versus v. We present them in figure 4. The decrease in S with decreasing v for small values of v (see the inset of figure 4) is related to the substantial sheet resistance increase with simultaneous constant slope of A versus v. Both $R_\square(v)$ and $S(v)$ curves are not convex in the region of v considered thus they cannot be approximated by the power laws typical of percolative behaviour (Bobran 1989, Bobran and Kusy 1989). We show below that the model of three-component 3D RRN can explain the characteristics considered with physically acceptable values of the network parameters.

Let us now briefly look inside the structure of the films investigated. The RuO_2–glass system is established as non-reactive (Vest 1975). When treating the parameters of the film sufficiently far from contact areas one has a quite well defined material: RuO_2 metallic-type crystallites embedded in a glassy matrix.

The projection of such a bulk material into a 3D RRN with three-point distribution of bond conductance: $g = 0, g = g_C, g = g_B$ seems to be well justified. In fact, the electrical conduction in a real film should take place via two types of bonds. The first, called metallic, is the high conductance bond ($g = g_C$ in the model), i.e. it appears for touching and/or sintered RuO_2 crystallites. The metallic conduction of RuO_2 grains indicates a positive temperature coefficient of resistance (TCR) (Ryden *et al* 1970, Kusy 1987). From

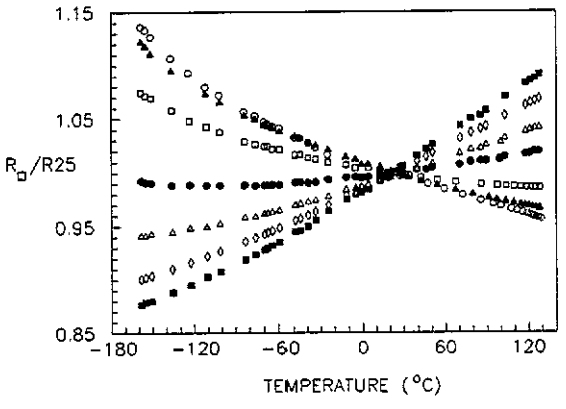

Figure 5. The set of temperature characteristics of resistance for RuO_2-based composites of v: (■) 0.32; (◇) 0.27; (△) 0.22; (●) 0.17; (□) 0.12; (▲) 0.08; (○) 0.05. R25 is the sheet resistance at the temperature 25 °C.

Kusy (1987) and Vest (1975), based on the knowledge of the mean diameter of a conducting grain, $\sigma = 400$ Å (we evaluated this from our surface area data for RuO_2), we state that the value of the resistance, r_C, of two sintered RuO_2 grains is of the order of 50 Ω. The second, MIM-type bond is poorly conducting ($g = g_B \ll g_C$ in the model) and occurs for every situation where the distance between two adjacent metallic grains is not so large as to disrupt the possible electrical conduction. It is assumed in our model that such a conduction originates from the direct thermally activated tunnelling. Some ideas on the formation of such structures in RuO_2-based TRFs have been given by Vest (1975), Sarma and Vest (1985) and Abe *et al* (1988b). The MIM-type bond has a negative TCR. The third, $g = 0$ bond conductance describes the remaining situations, i.e. the existence of non-conducting regions which have been observed by Vest (1975), Pike and Seager (1977), Prudenziati (1983), Kubovy (1986) and Gofuku *et al* (1989). This picture of the types of possible bonds can be assisted by recalling the following experimental argument. The shape of the temperature characteristics of resistance for TRF is paraboloidal thus showing the competition between the metallic-type (the positive slope of the curve) and the MIM-type (the negative slope) mechanisms of conduction (Pike and Seager 1977, Kusy 1979, Chen *et al* 1982, Inokuma *et al* 1984, Inokuma *et al* 1985, Kusy 1987, Kusy 1988, Abe *et al* 1988a, b). Abe *et al* (1988a) concluded that the parabola-like resistance versus temperature is an inherent characteristic of RuO_2-based composites. Figure 5 presents the set of $R(T)$ curves obtained for the composites investigated.

Let us consider the topological changes in a proposed model network due to the decrease in the fraction x of occupied sites. For sufficiently large x a metallic cluster exists spanning the electrodes. Next we reach the critical point x_c' at which the metallic cluster is cut off. The network still carries the current but MIM-type bonds begin to dominate. Finally x reaches the first critical point value x_c at which the conducting backbone is broken.

From the experimental arguments we find a similar behaviour in a real RuO_2–glass system. Resistance versus v is not convex in the range $\langle 0.02, 0.32\rangle$ of v but it is in the sub-region $\langle 0.02, 0.05\rangle$ and tends to be in the sub-region $\langle 0.08, 0.32\rangle$ (figure 4). Thus we can conclude the possible existence of two critical points v_c, v_c' corresponding to x_c, x_c' in the model. If one redraws the results of figure 4 into the sheet resistance–relative noise coordinates (figure 6) two distinct regions will be seen on the curve obtained. The first one, corresponding to v from 0.32 to 0.12 is roughly a straight line with the slope $w \simeq 2$. The other, looking like saturation of S versus $R_\square$ starts at $v = 0.12$ and ends at $v = 0.02$

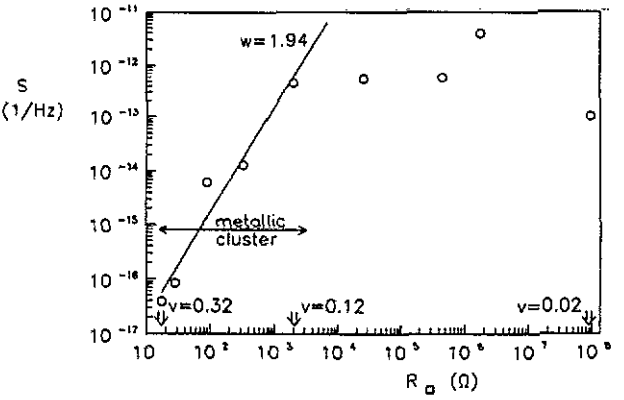

Figure 6. Relative noise S versus sheet resistance $R_\square$ for RuO_2–glass composites. Double arrows show the values of $R_\square$ corresponding to the characteristic values of v: 0.32 and 0.02 as the boundary values taken in the experiment and 0.12 as the approximate value for which we identify the cut-off of the metallic cluster. The solid line was obtained by the least squares power fit of experimental data for $0.32 \geqslant v \geqslant 0.12$.

as the lowest value used in the experiment. We attribute the different behaviour in the two regions to different mechanisms dominating the electrical conduction. As long as the metallic cluster exists, i.e. for $v \geqslant 0.12$ the TRFs show the metallic type of conduction. For $v \leqslant 0.12$ the metallic cluster breaks down and MIM-type bonds begin to carry the current. The strong argument confirming the last statement is the shape of the resistance versus temperature of figure 5. We obtained curves sloping upwards for $v > 0.17$ and downwards for $v \leqslant 0.12$ (see for comparison figure 4 of Kusy (1987)). Only the composite of $v = 0.17$ shows the negative slope of the characteristics for low temperatures and positive for higher ones. From the above considerations we state $0.12 \leqslant v_c' \leqslant 0.17$.

The first critical point, v_c, stands for the electrical conduction cut-off. We used the simple mathematical procedure of estimating v_c from the characteristics of $R_\square$ versus v (Lobb and Forrester 1987, Bobran and Kusy 1989). Starting from the fixed value of v_c less than but close to the lowest v taken from experimental data we decreased it by a constant amount with prior calculation of the pre-exponential factor and exponent t in the percolative resistance power law. We used the least squares fit method and continued the whole procedure until the minimum approximation quality factor was reached. Such a method was preceded by the choice of the critical region. We took into the fitting procedure only the points lying on the convex part of the $R_\square(v)$ experimental curve beginning from the lowest v (see figure 4). This way we obtained $v_c = 0.0149$ and $t = 2.10$.

More detailed description of the three-component 3D RRN model has been presented elsewhere (Kusy and Listkiewicz 1988, Kusy 1988, Kusy and Kolek 1989, Kolek 1989, Listkiewicz 1989). We consider here three of its parameters important for our discussion: $h_g \equiv g_B/g_C$, $h_s \equiv s_B/s_C$, where s_B and s_C are the relative noises of MIM-type bonds and metallic-type bonds, respectively, and b_1 which is the fraction of well-conducting bonds in the whole set of the conducting bonds. The value of h_g can be estimated from experimental data. Kolek (1989) proposed the method of h_g evaluation for three-component RRN on the basis of the analysis of his computer simulation results. He stated that the calculated resistivity ρ versus $(x - x_c)$ curves lie between the straight lines $\rho_B \propto h_g^{-1}(x - x_c)^{-t}$, corresponding to $b_1 = 0$, and $\rho_c \propto 1(x - x_c)^{-t}$, corresponding to $b_1 = 1$, in log–log scales, both with $t \simeq 2.0$. For values of $x \to x_c$ every characteristic approaches the first straight line, while for $x \to 1$ it approaches the second (see also Kusy and Kolek 1989). Referring the last statements to our experimental data, we used the following steps for h_g evaluation: (i) we redrew the experimental data as log $R_\square$ versus

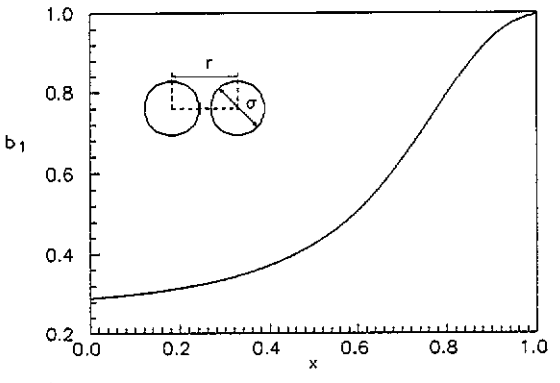

Figure 7. b_1 versus concentration of occupied sites x in a model where the volume fraction of hard spheres is $v = x \times f$ and $f \simeq 0.66$ is the random close-packing factor.

$\log(v - v_c)$; (ii) the changes of $R_\square$ found for $0.02 \leqslant v \leqslant 0.32$ were 10^8 (see figure 4); (iii) according to the power law, increasing v from 0.02 to 0.32 causes a decrease in the resistance by a factor $10^{4.5}$ (Bobran and Kusy 1989). So we conclude that $h_g \simeq 10^{-3.5}$. Taking into account that $r_C \simeq 50\ \Omega$ as mentioned previously we obtain the value of poorly conducting bond resistance $r_B \simeq 160\ \text{k}\Omega$. The last result agrees with that obtained by Kusy (1987).

We interpret b_1 as the number that for TRF reflects the processes of microstructure development (it can be called the sintering coefficient), so in practice it is influenced by technological parameters. As v becomes smaller some electrical bonds from a set of good conductors should fall into the poorly conducting group and some from the latter should break and fall into the $g = 0$ group. We say that for RRN b_1 must be x-dependent. For a first approximation $b_1(x)$ can be evaluated based on the nearest-neighbour distribution function $H(r)$, i.e. the probability density corresponding to finding a nearest neighbour at some given distance r from the reference particle in a continuous 3D system of hard spheres of diameter σ. This probability density function has been calculated by Torquato *et al* (1990). If we assume that the thermally activated tunnelling is the mechanism of electrical conduction through MIM structures then the thickness of insulating barriers should not be greater than about 20 Å. Next, we have to maintain $b_1 \simeq 1$ for the volume fraction of hard spheres to be equal to the random close-packing factor $f \simeq 0.66$, as only touching particles exist in such a system. Thus we define

$$b_1(x) \equiv \int_1^{1.015} \sigma H(r/\sigma, x)\, \mathrm{d}(r/\sigma) \Big/ \int_1^{1.05} \sigma H(r/\sigma, x)\, \mathrm{d}(r/\sigma). \tag{4}$$

We show the plot of $b_1(x)$ given by (4) in figure 7.

Taking into account both the value of $h_g = 10^{-3.5}$ approximated from experiment and the assumed $b_1(x)$ dependence we performed computer simulations of three-component RRN using the real space renormalization group (RSRG) algorithm (Kolek 1989, Kusy and Kolek 1989). Using this algorithm we calculated S versus the network resistivity, ρ, for $h_s = 1, 10, 10^2, 10^3, 10^4$ and 10^5. The results are presented in figure 8. It is seen that for $h_s = 10^3$ we obtained the curve that in a certain range of ρ qualitatively fits the experimental $S(R_\square)$ data (see figure 6). In fact, the simulation data yield an almost straight line dependence of S versus ρ with the slope $w \simeq 2$ for $2 \times 10^1 \leqslant \rho \leqslant 10^3$ and a weak function of S versus ρ for $10^3 \leqslant \rho \leqslant 3 \times 10^4$. For higher values of resistivity, S again increases. Qualitatively the same behaviour of $S(R_\square)$ is easily identified for our

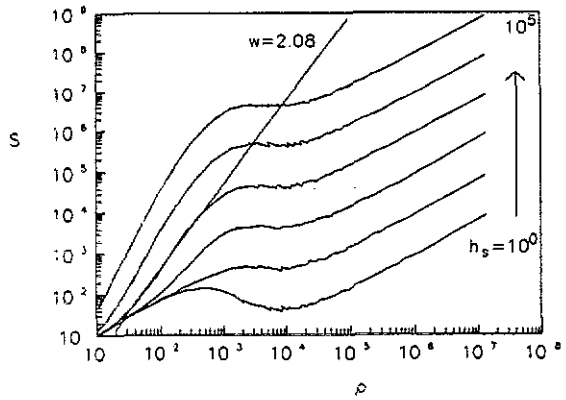

Figure 8. Relative noise S versus resistivity ρ for three-component 3D RRN. The lines are the results of RSRG computer simulations for $h_g = 10^{-3.5}$, $b_1(x)$ given by (4) and $h_s = 1$; 10; 10^2; 10^3; 10^4; 10^5. We assumed $g_C = 1$, $g_B = h_g$, $s_C = 1$, $s_B = h_s$ in the model. The solid line of slope $w \simeq 2$ is the result of the least squares power fit of simulation data for $2 \times 10^1 \leq \rho \leq 10^3$.

experimental data of figure 6. Based on the above considerations we postulate that the MIM-type bond in TRF has a relative noise one thousand times greater than the metallic-type one. We cannot explain the course of the experimental curve for the highest resistance point. This discrepancy can be due to a b_1 versus x dependence other than the proposed one. Perhaps b_1 should be equal to zero for small x and start to be greater than zero for x sufficiently large. On the other hand, the experimental point $S(v = 0.02)$, $R_\square(v = 0.02)$ lies close to the percolation threshold v_c and therefore probably undergoes quite large scatter.

4. Conclusions

The influence of CMPFs on the measured characteristics of RuO_2–glass composite has been eliminated. The estimated characteristics of $R_\square(v)$, $R_\square(T)$, $S(R_\square)$ allowed us to approach the microstructure and electrical transport by the three-component 3D RRN. It turned out that the proposed model possesses the reasonable physical interpretation of its parameters and yields a qualitative fit to our experimental data. For TRFs we found and interpreted two critical points: v_c' being the volume fraction of conducting component for which the metallic cluster is cut off and v_c for which the electrical conduction is broken. As a result of our research we obtained $v_c \simeq 0.0149$ and v_c' in the range of 0.12 to 0.17. The second percolation threshold is not clearly visible on the characteristics of $R_\square$ versus v but it appears on the relative noise versus $R_\square$ curve. It can also be recognized from the temperature characteristics of resistance. It turned out that while a well conducting bond has a resistance of the order $r_C \simeq 50\ \Omega$ then the poorly conducting bond has one of the order $r_B \simeq 10^5\ \Omega$. We have also observed the best fit to the experimental data by the results of computer simulations for $h_s = 1000$.

The future experimental work on the subject will take into consideration more numerous compositions of RuO_2–glass including different crystallite sizes of the metallic component. We will concentrate on the measurement of electrical parameters for TRFs of compositions close to the percolation threshold. Further investigation of b_1 versus x will also be carried out to improve the fit of the experimental data and Monte Carlo computer calculations.

Acknowledgments

The authors are grateful to A Kolek for useful discussions on the three-component RRN percolation model and to S Paszczyński for a potential probe used in measuring the potential distribution. We are also grateful to all participants in the cycle of PhD seminars by one of us (AK) for remarks during our work on the paper. This paper has been financially supported by the Polish Government Central Program of Fundamental Research CPBP 02.14 and by the Technical University of Rzeszów Research Task B-172.

References

Abe O, Taketa Y and Haradome M 1988a *Thin Solid Films* **162** 7–12
—— 1988b *Active Passive Electron. Components* **13** 67–83
Bobran K 1989 *Z. Phys.* B **75** 507–11
—— 1990 *Proc. 13th Conf. of the International Society for Hybrid Microelectronics–Poland Chapter* (Wrocław: ISHM—Poland Chapter) pp 129–32
Bobran K and Kusy A 1989 *Proc. 12th Polish Conf. Circuits Theory and Electron. Net., Rzeszów-Myczkowce* (Rzeszów: Widawnicta Politechniki Rzeszowskiej) vol 2, pp 437–42 (in Polish)
Carcia P F, Suna A and Childers W D 1983 *J. Appl. Phys.* **54** 6002–8
Cattaneo A, Cocito M, Forlani F and Prudenziati M 1977 *Electrocomp. Sci. Technol.* **4** 205–11
Chen T M, Su S F and Smith D 1982 *Solid State Electron.* **25** 821–7
deJeu W H, Geuskens R W J and Pike G E 1981 *J. Appl. Phys.* **52** 4128–34
Demolder S, Van Calster A and Vandendriessche M 1983 *Electrocomp. Sci. Technol.* **10** 81–5
Demolder S, Vandendriessche M and Van Calster A 1980 *J. Phys. E: Sci. Instrum.* **13** 1323–7
Feng S, Halperin B I and Sen P N 1987 *Phys. Rev.* B **35** 197–214
Gofuku E, Ogama T and Takasago H 1989 *J. Appl. Phys.* **66** 6126–31
Halperin B I, Feng S and Sen P N 1985 *Phys. Rev. Lett.* **54** 2391–4
Inokuma T, Taketa Y and Haradome M 1984 *IEEE Trans. Comp. Hybrids Mfg. Technol.* CHMT-7 166–75
—— 1985 *IEEE Trans. Comp. Hybrids Mfg. Technol.* CHMT-8 372–3
Kolek A 1989 *PhD Thesis* Technical University of Warsaw (in Polish)
Kolek A and Kusy A 1988 *J. Phys. C: Solid State Phys.* **21** L573–8
Kubovy A 1986 *J. Phys. D: Appl. Phys.* **19** 2171–83
—— 1988 *Silikaty* **32** 289–303
Kusy A 1979 *Structure, conduction mechanisms and 1/f noise in thick resistive films* (Rzeszów: Wydawnicta Politechniki Rzeszowskiej) (in Polish)
—— 1987 *J. Appl. Phys.* **62** 1324–34
—— 1988 *Proc. Int. Conf. Ceramics for Electronics, Pardubice* 148–63
Kusy A and Kolek A 1989 *Physica* A **157** 130–4
Kusy A and Listkiewicz E 1988 *Solid-State Electron.* **31** 821–30
Listkiewicz E 1989 *PhD Thesis* Technical University of Warsaw (in Polish)
Listkiewicz E and Kusy A 1985 *Thin Solid Films* **130** 1–15
Lobb C J and Forrester M G 1987 *Phys. Rev.* B **35** 1899–1901
Mantese J V and Webb W W 1985 *Phys. Rev. Lett.* **55** 2212–5
Müller F and Wolf M 1988 *Active and Passive Elec. Comp.* **13** 1–6
Paszczyński S 1985 *Electrocomp. Sci. Technol.* **12** 71–89
Pike G E 1978 *AIP Conf. Proc.* **40** 366–71
Pike G E and Seager C H 1977 *J. Appl. Phys.* **48** 5152–69
Prudenziati M 1983 *Electrocomp. Sci. Technol.* **10** 285–93
Rhee J G and Chen T M 1978 *Solid State Technol.* **21** 59–62
Ringo J A, Stevens E H and Gilbert D A 1976 *IEEE Trans. Parts, Hybrids Pack.* **PHP-12** 378–80
Ryden W D, Lawson A W, Sartain C C 1970 *Phys. Rev.* B **1** 1494–1500
Sarma D H R and Vest R W 1985 *J. Am. Ceram. Soc.* **68** 249–53
Stauffer D 1985 *Introduction To Percolation Theory* (London: Taylor and Francis) pp 52, 87–91
Torquato S, Lu B and Rubinstein J 1990 *J. Phys. A: Math. Gen.* **23** L103–7

Tremblay A M S, Feng S and Breton P 1986 *Phys. Rev.* B **33** 2077–80
Tremblay A M S, Fourcade B and Breton P 1989 *Physica* A **157** 89–100
Vest R W 1975 *Conduction mechanisms in thick-film microcircuits* (Purdue Final Technical Report, ARPA Order 1642) (unpublished)
Yamaguchi T and Kageyama M 1988 *IEEE Trans. Comp. Hybrids Mfg. Technol.* **11** 134–6